ISSN 1063-7729, Astronomy Reports, 2006, Vol. 50, No. 5, pp. 411–421. © Pleiades Publishing, Inc., 2006.
Original Russian Text © V.M. Grigor'ev, L.V. Ermakova, A.I. Khlystova, 2006, published in Astronomicheskiĭ Zhurnal, 2006, Vol. 83, No. 5, pp. 464–474.

Evolution of a Filament Due to Magnetic-Field Variations in a Complex Active Region

V. M. Grigor'ev, L. V. Ermakova, and A. I. Khlystova

Institute of Solar—Terrestrial Physics, Siberian Division, Russian Academy of Sciences, P.O. Box 4026, Irkutsk, 664033 Russia

Received July 13, 2005; in final form, November 14, 2005

Abstract—The complex active region NOAA 9672 is studied when it was near the central meridian, from October 21—26, 2001. At that time, there was an emergence of new magnetic flux, with the ongoing formation of a filament. The dynamics of the magnetic field are studied in order to search for their possible manifestations in the filament structure, using SOHO MDI magnetograms, SOHO EIT and TRACE filtergrams in the 171 Å line, and Hα filtergrams available via the Internet. Our earlier conclusion that filaments form at the boundaries of supergranules near polarity-inversion lines is confirmed. The conclusion of Chae that sinistral filaments have positive magnetic helicity is also confirmed. New information about magnetic-field decay processes is obtained. The direction of motion of the magnetic poles and their relative positions suggest that the axial field of a filament forms as a result of either reconnection of cancelling magnetic poles, or emergence of horizontal magnetic-flux tubes.

PACS numbers : 96.60.R
DOI: 10.1134/S1063772906050106

1. INTRODUCTION

In recent years, the relation of the dynamics of photospheric magnetic fields to the structure and evolution of filaments has been intensely studied (see, e.g., [1—4]). Along with the influence of the large-scale dynamics of the magnetic field, small-scale processes such as magnetic-flux cancellation have been considered. Cancellations were discovered 20 years ago [5, 6] and were defined as a true pairwise disappearance of the magnetic flux of two colliding regions of the magnetic field with opposite polarities. The approach of regions of opposite polarity results in unusually high horizontal gradients of the longitudinal field. The rate of flux disappearance is 10^{18} Mx/h for the quiet Sun and 10^{19} Mx/h or more for active regions. Harvey et al. [7] analyzed the data for five levels of the nonturbulent solar atmosphere in order to determine whether the magnetic flux moves upward or downward as a result of the cancellation. They concluded that, in most cases, a bipolar group is pulled downward. Considerable evidence on the important role of cancellation in the formation and maintenance of filaments has been obtained. There is no doubt that there is a relationship between the origin and growth of filaments and magnetic-flux cancellations, though the mechanisms involved have not been definitely established. Movies [8] composed from Hα filtergrams and longitudinal-field magnetograms obtained at the Big-Bear Solar Observatory convincingly demonstrate the relationship of a filament with magnetic-flux cancellation. The mutual positions of the filament and pair of cancelling magnetic structures are such that one end of the filament seems to emerge from the contact of the cancelling opposite polarities. Furthermore, the motion of the material toward the opposite end of the filament is clearly visible. This indicates that a cancellation process is involved in the formation of the filament magnetic field and the accumulation of material in the filament.

Measurement of the magnetic fields from space enables a continuous observation of the studied magnetic objects, making it possible to reconstruct a full picture of their development and establish the history of structural changes in filaments or filament formation. In the current paper, we continue to study the effect of magnetic-field dynamics on filament formation and stability, based on SOHO MDI data.

2. OBSERVATIONAL DATA AND OBJECT OF THE STUDY

We analyzed the development of a filament in the active region NOAA 9672, which was observed on the solar disk from October 17 to October 29, 2004, within a long-lived activity complex (AR NOAA 9672+9670) in its fourth transit. This region was located in the southern hemisphere at a

Log of Hα filtergrams

Date (October 2001)	UT
21	07:16, 10:28
22	04:08, 07:10, 08:40, 14:37, 16:55, 18:00, 19:00, 20:00, 21:00, 22:00, 23:00, 23:25
23	07:12, 08:00, 15:04, 16:00, 17:00, 18:00, 19:00, 20:00, 21:00, 22:00, 23:00, 23:20
24	00:01, 02:52, 07:57, 16:00, 17:00, 18:00, 19:00, 20:00, 21:00, 22:00, 23:00, 23:10
25	03:01, 09:43, 16:18, 16:59, 18:00, 18:25, 20:00, 21:00, 22:00, 23:00
26	00:02, 03:10, 06:00, 07:52, 16:15

latitude of $\sim 16°-26°$. A new magnetic flux emerged in the active region NOAA 9672 from October 20–25, accompanied by powerful active processes. This active region produced several strong flares (the most powerful on October 22 at 17:59 UT (X1/2b) and on October 25 at 15:02 UT (X1/2b)), accompanied by coronal ejections.

We used SOHO MDI magnetograms of the longitudinal magnetic field, SOHO EIT filtergrams, and TRACE 171 Å and Hα filtergrams available over the Internet. The magnetograms were taken every 96 min and had a spatial resolution of 2″. Big-Bear hourly filtergrams are available from 16:00–23:00 UT. During the rest of the day, there were occasional filtergrams of other observatories. The times of all the Hα filtergrams used are listed in the table.

We considered the interval from October 21 to 26, when the central part of the active region was at longitudes 40E–35W. The time resolution of the data used enables us to draw conclusions about the main stages of the life of a filament as a whole; the timescale accessible to interpretation is limited to tens of minutes, and the spatial scale to several thousands of kilometers.

Figure 1a shows an MDI magnetogram, with contours of filaments and a sunspot umbra plotted using the Hα filtergram. A field of negative polarity is surrounded on the west, north, and east by a field of positive polarity. A considerable number of the lines of force enters the center. By the beginning of the interval considered, the active region contained a large sunspot with negative polarity (the leading polarity in the southern hemisphere for the current cycle). There is a $\cap$-shaped filament to the north of the sunspot, and a quiescent filament oriented in the EW direction is located to the southeast of the active region. As it reaches the active region, this filament turns to the north along the eastern polarity-inversion line and ends to the south of the sunspot. Another filament is at the western polarity-inversion line. The events considered took place in the eastern part of the active region. On the first four days, new magnetic flux emerged on and to the southwest of the sunspot site. A delta configuration was formed on the sunspot, with the sunspot area more than doubling.

3. RESULTS AND DISCUSSION

3.1. Evolution of the Filament

Figure 2 presents the Hα filtergrams. Our analysis shows that we can consider the filaments at the eastern polarity-inversion line within and behind the active region to be a single structural formation, whose shape changes in accordance with the particular magnetic conditions acting. The filament channel expands in the region of weak magnetic fields and shrinks in the region with a high magnetic-flux density. The filament structure in the region of the weak magnetic fields, which is visible on many of the filtergrams, tells us that the filament belongs to the sinistral type, as is typical of the southern hemisphere. Following the rule for finding the direction of the axial magnetic field of a filament [9], we obtain the direction shown in Fig. 1a for filaments of this type and for the given magnetic field distribution. Extending this to a $\cap$-shaped filament, we obtain an agreement between the filament arrangement with respect to the magnetic-field polarities, namely, the eastern end of the filament is connected to the positive field, and the western end to the negative field. The tilt of the dark elongated structures above the sunspot penumbra on the Hα filtergrams, as well as the tilt of the $\cap$-shaped filament, suggest clockwise sunspot rotation, as is typical for this hemisphere. Figure 1 shows also the SOHO EIT 171 Å filtergram obtained on October 22 at 13:00 UT, with the corresponding MDI magnetogram. The orientation of the loops that cross the eastern polarity-inversion line suggests the presence of a shear configuration of the magnetic field; the direction of the shear field coincides with that of the field in a sinistral filament.

According to the available Hα filtergrams and without considering the disappearances of filaments

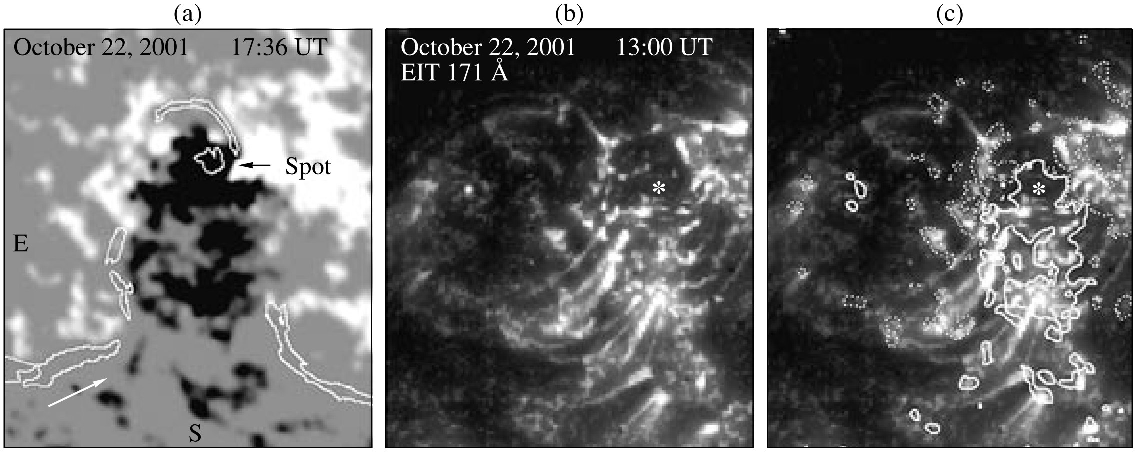

Fig. 1. (a) MDI magnetogram with contours of filaments and spot umbra. White and black represent positive and negative polarity, respectively, while the white arrow represents the direction of the axial magnetic field in the filament. (b) EIT 171 Å filtergram. The asterisk shows the sunspot center. (c) Superposition of magnetic-field contours on the EIT 171 Å filtergram; see text.

in flares, the chronology of the main events related to the filament is the following:

October 22 19:00–20:00 UT: appearance of a new part of the filament;

October 23 18:00 UT: beginning of the separation of the filament into two parts, inside and outside the active region;

October 24 21:00 UT: disappearance of the meridional part of the filament in the active region, with the subsequent recovery by October 25;

October 25 02:44 UT: filament activation.

Let us consider these changes in more detail. The middle part of the filament was first observed on October 22, after the termination of a powerful X-ray flare, and looked like a narrow structure passing along the boundaries of two cells of the chromospheric network (shown by an arrow in Fig. 3). It was already visible at 16:55 UT, and at subsequent times as a narrower and less contrasting structure with sharp edges; only in the first frame its central part is slightly shifted to the west of the chromospheric cell boundaries. In her description of the formation of a small filament in a decaying small active region, Martin [10] pointed out that this was preceded by the emergence of parallel, continuously changing dark strands in Hα, which gradually accumulated absorbing material; this entire process took a quarter of an hour. Our case of high magnetic flux density is characterized by the stability of the position and shape of the "prefilament," and by a longer time scale.

On October 23 at about 18:00 UT, the filament separated into two parts, one inside and one outside the active region, with this separation persisting until October 26. The filaments ended at the boundaries of a cell of the chromospheric network; i.e., they were located on either side of a supergranule. From approximately the same time, the ∩-shaped filament appeared to be part of the active-region filament. On October 24 at 21:00–24:00 UT, the meridional part vanished, and only the ∩-shaped filament remained; there were no flares at that time. At the beginning of the next day, the filament restored to its previous form.

3.2. Sign of the Filament Chirality

The rope structure of the filament is visible in the second-to-last frame of Fig. 2, obtained on October 25 at 03:01 UT at the Learmonth Observatory. Figure 4 shows this filtergram on a larger scale, with a TRACE 171 Å map. This somewhat unusual appearance of the filament is due to the process of activation (see below). If we look in the direction of the axial magnetic field, the ropes are twisted clockwise; consequently, the magnetic helicity in the filament is positive. The twist is about half-turn. Chae [11] used EUV maps obtained by TRACE at 171 Å to determine the sign of the filament chirality. By isolating individual threads in filaments and analyzing their intersections, Chae determined the sign of the chirality for two dextral and one sinistral filament, and concluded that dextral and sinistral filaments have negative and positive magnetic chirality, respectively. Filament threads are usually not visible in Hα filtergrams, but, in our case, larger structures became visible during activation; the sign of their chirality probably coincides with that of the threads.

3.3. Evolution of the Magnetic Field in the Active Region

The MDI magnetograms yield information about the longitudinal magnetic field; i.e., the line-of-sight

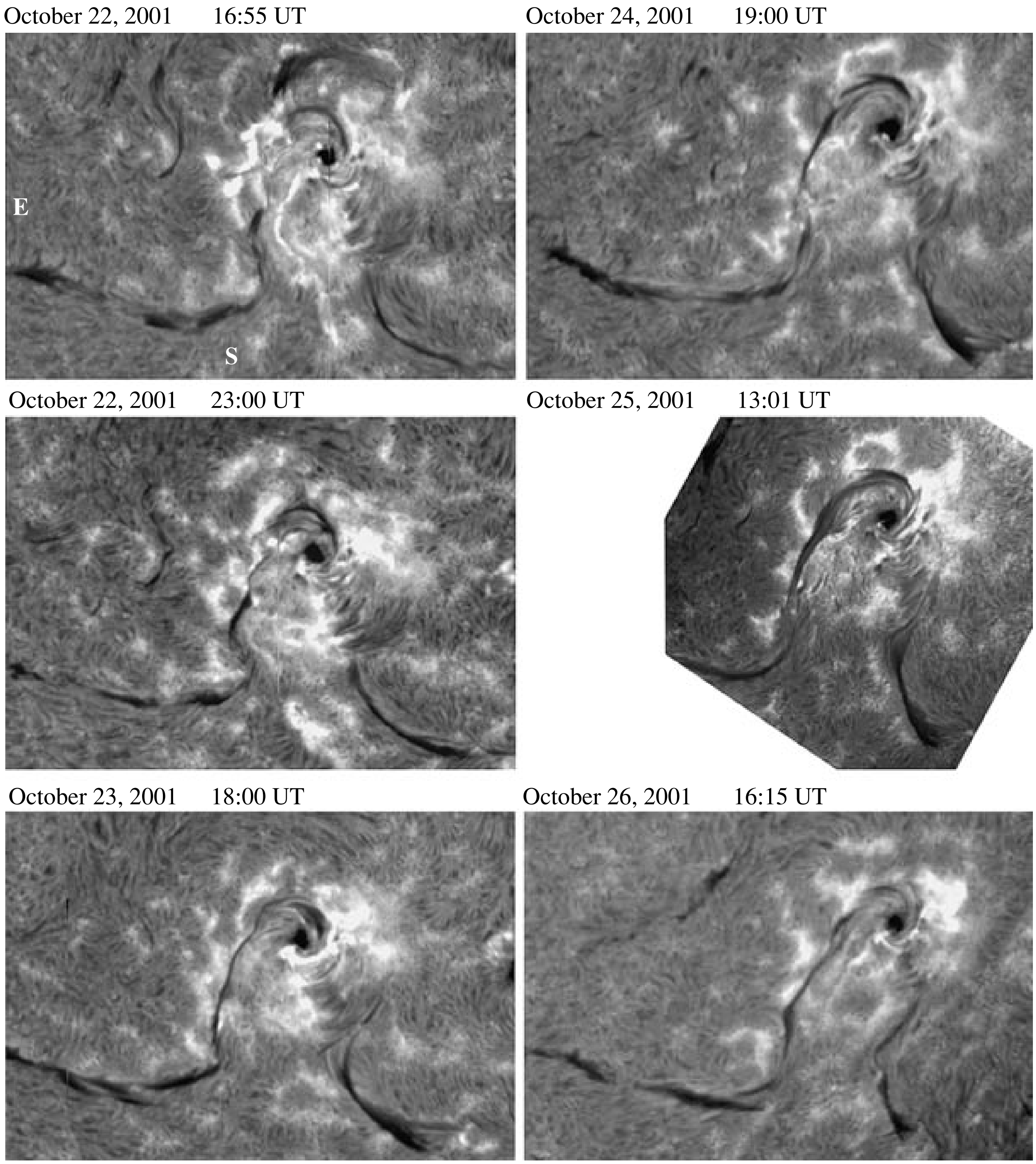

Fig. 2. Evolution of a filament in the active region NOAA 9672 in Hα filtergrams.

component of the magnetic-field vector. In the central heliolongitude zone ($\pm 30°$), where the active region was from October 22–26, the longitudinal field differs little from the vertical component. Using IDL, we rotated the magnetic maps to the central meridian to enable a direct superposition of the maps, thus eliminating foreshortening of the perspective. Further, we cut out the fragment that contained the active region and its vicinity.

Figure 5 shows a sequence of MDI magnetograms. Intense motions are observed in movies composed of these magnetograms. As was already mentioned, the magnetic-field configuration in the active region is somewhat unusual: many umbras sunspot at the center of the active region determines the pattern and character of the motions. The dominating form of motion of the magnetic field, with leading and trailing polarity, in the eastern half of the active region that is of interest for us was away from the sunspot with a counterclockwise displacement. The trajectories of motions formed ringlike structures with supergranular size, as well as considerably

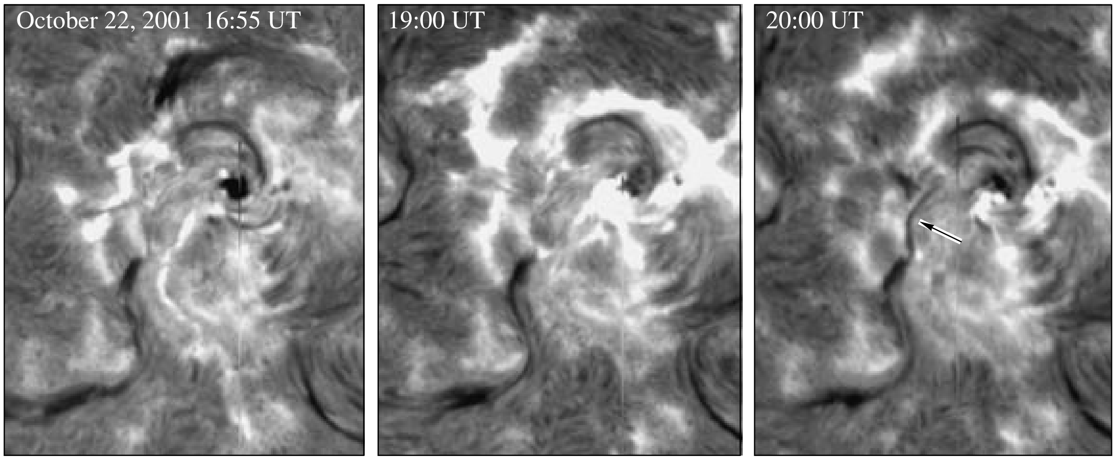

Fig. 3. Formation of a new fragment of the filament in the Big-Bear Hα filtergrams.

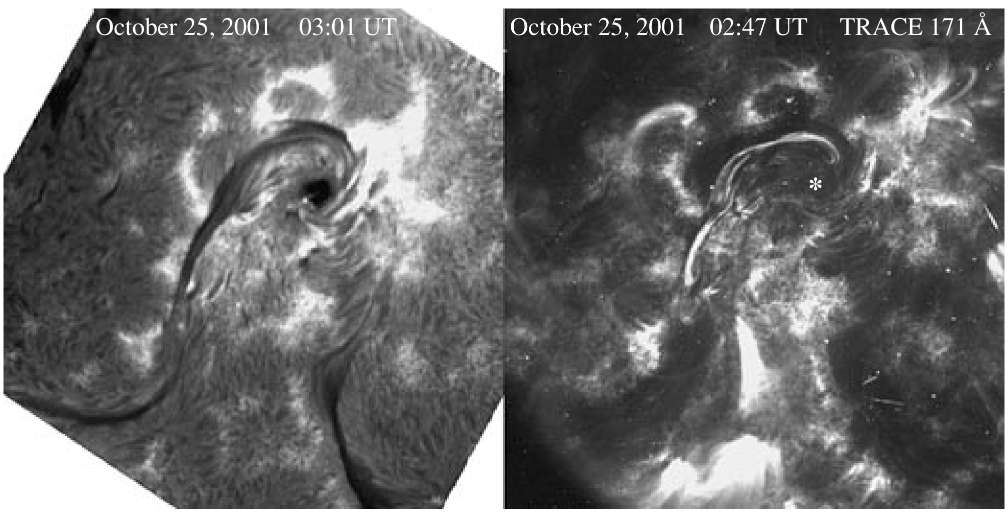

Fig. 4. Filtergrams in the Hα and FeIX and X 171 Å lines displaying the development of the filament structure during its activation. The asterisk on the TRACE 171 Å filtergram shows the sunspot center.

smaller ones, with diameters of ∼10 000 km. This was especially clearly visible in the field of negative polarity that was "squeezed" from three sides by a field of positive polarity. These small ringlike structures were most pronounced on October 24 and 25, when the magnetic flux reached its maximum. Some cells were traced by the motion of the fields from two sides towards each other. The apparent speed of the motion occasionally exceeded 1 km/s. The lifetimes of the dynamic structures were from several hours to several tens of hours. Their size is too small for supergranules, though Zwaan [12] noted that supergranules in active regions are smaller, and Shine et al. [13] associated similar scales, 5–10 thousand km, with small supergranules. The motion of the magnetic field along the cell boundaries proceeded, as a whole, toward lower magnetic flux densities, so that the magnetic field on the considered polarity-inversion line was moving southward. At the end of the interval when the magnetic flux began to decrease, the intensity of the motions diminished. By 05:00–08:00 UT on October 26, a "moat" was formed around the multipolar sunspot on its north and east sides, and the motions in the sunspot appeared to be a continuation of the previous ones. This moat had an unusual feature: its boundary was delineated by magnetic fields with the opposite sign to the sunspot field. The formation of the moat signals the completion of the sunspot formation. There is a field of positive polarity at the eastern polarity-inversion line, which is basically old and fragmented, and is less dynamical than the negative-polarity field. Most of this positive field is enclosed within the active region. The negative field grew appreciably during the interval considered,

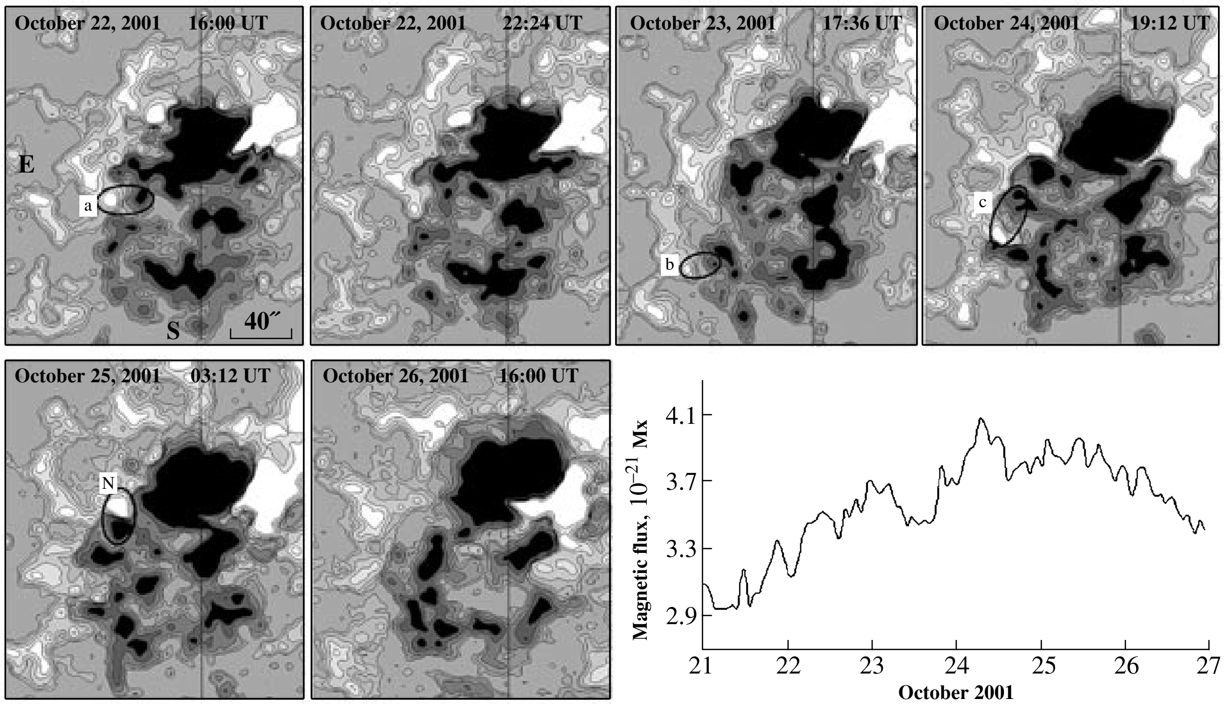

Fig. 5. MDI magnetograms showing the evolution of the active region; the bipolar magnetic pairs ("a," "b," and "c") and the N segment are outlined. The vertical line divides the region into eastern and western parts. The flux variation of the positive magnetic field (white in the magnetograms) in the eastern part is shown.

and a new flux emerged, associated mainly with the northwest and west fields of positive polarity.

It is not possible to isolate the negative magnetic flux that is closed through the eastern polarity-inversion line of interest for us. Therefore, we will restrict our analysis to the dynamics of the positive flux for the eastern part of the magnetograms (Fig. 5). This flux grew considerably from October 21–25; i.e., the formation of the filament took place against a background of increasing magnetic flux. The observed fluctuations of the flux may be related to short-lived local processes, the emergence of new bipolar pairs, or cancellations.

3.4. Local Magnetic Events

It is difficult to identify emerging bipolar pairs. It is not always possible to confirm the relation between supposed members of a pair using filtergrams, partially because filtergrams are not available for the required time. Whether two new magnetic poles form a bipolar pair can be judged on the basis of their dynamics: simultaneous emergence, their positional relationship, the magnitude of the magnetic flux, general tendencies in their development, and similarity in their motions. Subsequently, the components of a pair can interact with other elements (even more than one). The formation of a new magnetic hill and an increase in flux are taken to signal the emergence of a new magnetic tube. We have selected four of the strongest local magnetic events: three cases of the emergence of new magnetic flux with subsequent cancellation of one of the bipolar pair components, and a case of decreasing magnetic fluxes with ages of no less than two to three days, whose previous dynamics were more complicated. These events are consistent with key changes in the filament.

Formation of a new part of the filament on October 22. We can relate this event to the emergence of bipolar magnetic pair "a," whose positive component moved southward, came across an older negative magnetic pole, and was cancelled (site I). Figure 6 shows fragments of magnetograms and Hα filtergrams illustrating the dynamics of the process. This figure also shows the flux variation of the positive component in the bipolar pair. If the cancelled magnetic poles had no topological connection, cancellation should result in the reconnection of the magnetic-field lines. If we suppose that the above mentioned negative pole was closed on some positive pole to the east of it, in accordance with the shear configuration inferred by the EIT 171 Å filtergrams (Fig. 1), cancellation would move this shear configuration northward, to the site where the new part of the filament formed. According to the graph in Fig. 6, the magnetic flux decrease due to

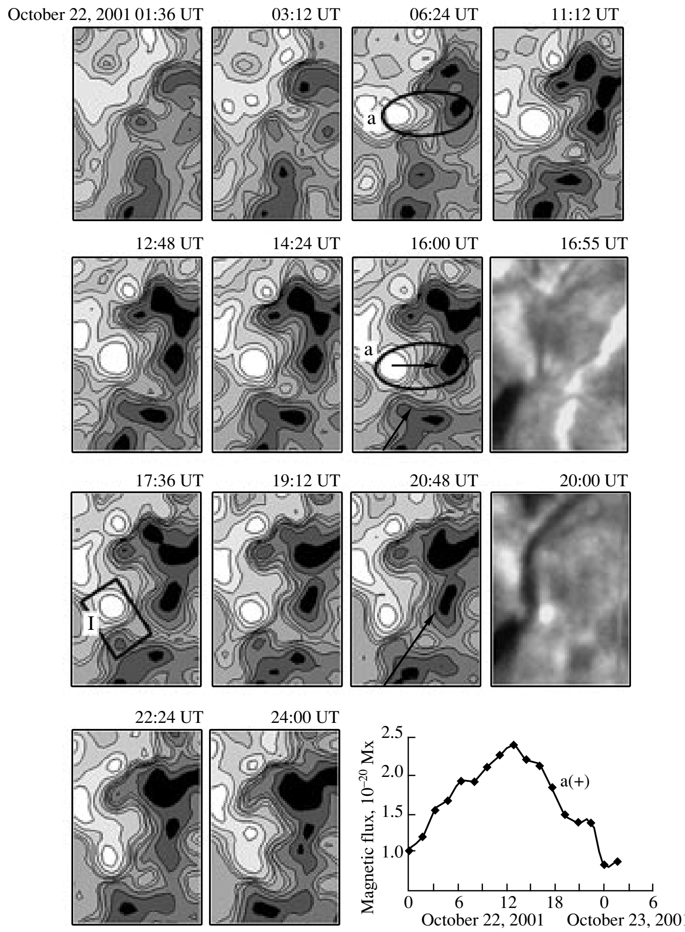

Fig. 6. Development of bipolar magnetic pair "a" and flux cancellation site I. MDI magnetograms and Hα filtergrams are shown. The arrows show the supposed direction of the magnetic field before cancellation. The change in flux of the positive component is shown; the curve is labeled with the symbol of the bipolar pair and the sign of the magnetic field.

the cancellation began in the afternoon. As noted in Section 3.1 and follows from Fig. 6, the outline of the future filament is already visible in the Big-Bear Hα filtergram obtained at 16:55 UT.

Separation of the filament into two parts. The filament separated into a filament inside the active region and another outside of it, as is illustrated in Fig. 7. At the end of the day on October 23, new magnetic flux emerged at the periphery of the active region, the bipolar pair "b," the archlike filament systems are visible on the Hα filtergrams. The axis of the bipolar pair was directed across the filament, and the filament was broken. The second bipolar magnetic pair "c" emerged farther to the north; its positive component moved southward and came across the negative pole of bipolar pair "b," leading the two poles to cancel. Reconnection of the negative pole of pair "b" to the positive pole of pair "c" caused the creating of a magnetic field directed along the filament (Fig. 7). The filament was separated on the boundary between the active region and the surrounding fields. The former magnetic configuration was "ripped apart." In the next two days, the negative protrusion on the polarity-inversion line was cancelled, and the filament channel again became continuous.

Activation of the filament. According to the data of the Hida Observatory (Japan) presented on the Internet, a so-called IIC phenomenon was observed on October 25 at a site with coordinates S19 W11. This is, by definition, a transient dark structure identified with some activation or disappearance of a preexisting filament. There was no eruption of a filament. This region contains one of the sites of magnetic flux decrease we have found (labeled N in Fig. 5); the middle part of the filament lies above it. According to the TRACE 171 Å filtergrams, a brightening appeared above this site at 02:42 UT; which then spread to both ends of the filament. The series of filtergrams shows the consecutive appearance of bright thread-like structures that trace the filament. Short bright parallel structures to the west of the middle part of the filament (Fig. 4) testify to the magnetic connection of

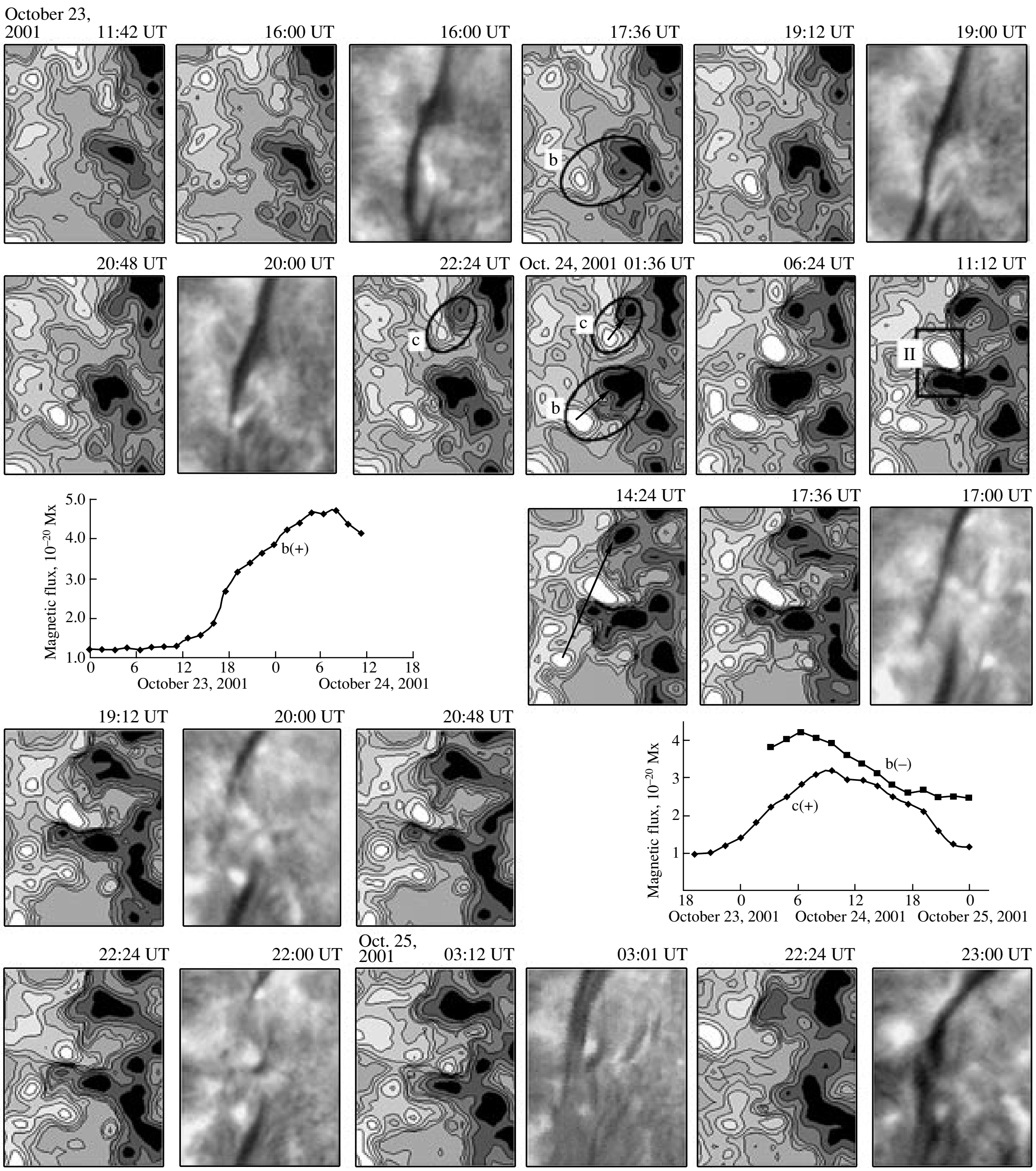

Fig. 7. Development of bipolar magnetic pairs “b” and “c” and cancellation site II. MDI magnetograms and Hα filtergrams are presented. The arrows show the supposed direction of the magnetic field before the cancellation. Variations of the absolute value of the flux are shown. Left: increasing positive flux of bipolar pair “b,” which “tore” the filament. Right: cancelling fluxes (positive and negative). The notation is the same as in Fig. 6.

the positive pole of site N with the adjoining negative sunspot field. Figure 8 illustrates the dynamics of the magnetic field. During the day, the positive pole virtually disappeared. The site-N negative pole located to the south also weakened considerably. The variation of the positive magnetic flux is shown in a separate panel. According to the vector magnetogram, the magnetic fields of the positive and negative poles are perpendicular to each other. A decrease of positive flux occurred not only on the southern side, where the magnetic-field gradients were highest, but also on the western side, where the positive pole was closed on the sunspot. This may be due to the submergence of a magnetic loop. The dynamics of the negative field in the western part of the magnetograms during 03:12–16:00 UT is consistent with this. Summarizing the basic parameters of this site, it has a considerable size along its major axis (30 000 km),

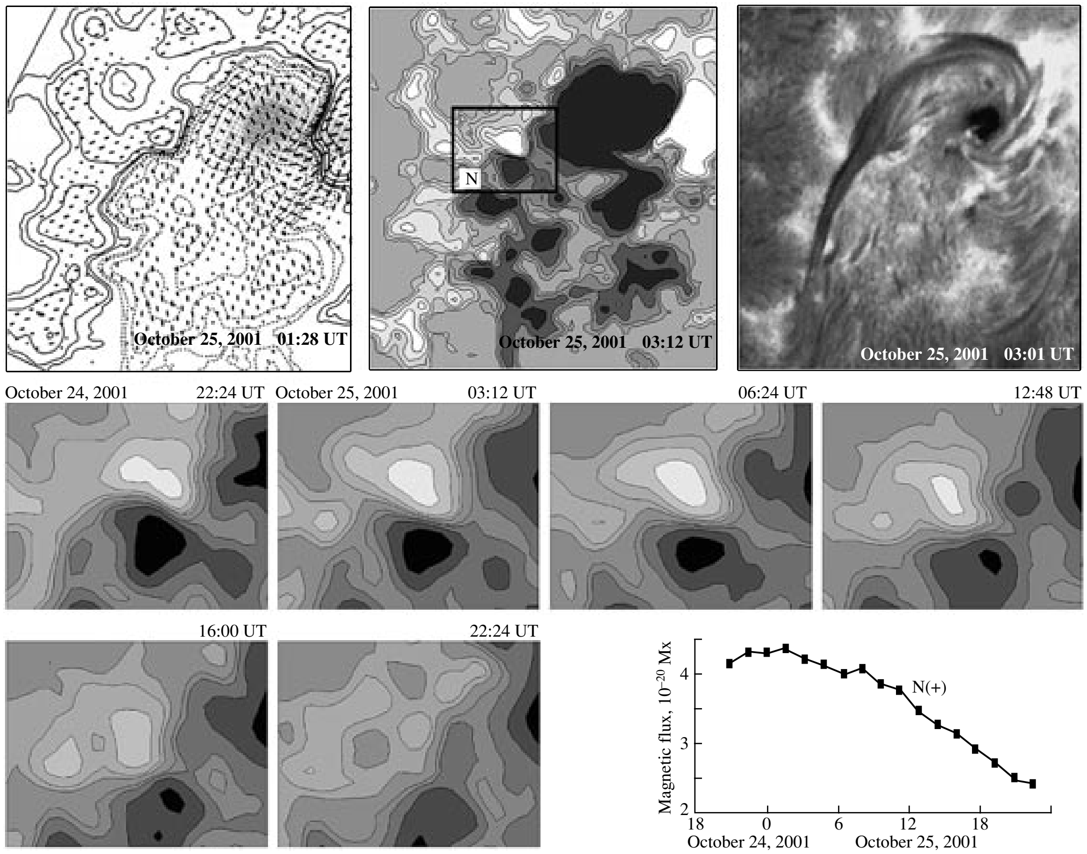

Fig. 8. Dynamics of the magnetic field on site N. The upper row shows the vector magnetogram, MDI magnetogram, and the Hα filtergram for the entire active region. Below are shown fragments of MDI magnetograms, including site N, and the variation of the flux of the positive component.

a high magnetic-flux density, intersecting magnetic fields, and a decrease in the magnetic flux of both polarities. The filament activation coincided with the beginning of the decrease in the positive magnetic flux. The described event is a fragment of a more prolonged event. On October 21–22, this pole was located to the north and had a common penumbra with the sunspot; it then tore off from the sunspot and, moving to the southeast, reached a large negative pole by October 24. The pattern of high magnetic-field gradients observed since then, which is typical of cancellations, existed for two days, finally ending in the disappearance of the poles of both signs (Fig. 5, last frame). The motion of the positive pole may be a manifestation of a magnetic tube twisting. The vector magnetogram of the National Astronomical Observatory of Japan [14] shows that the negative magnetic field in the sunspot is twisted clockwise. This also follows from the Hα filtergrams (see Section 3.1). Brown et al. [15] demonstrated the rotation of sunspots using TRACE data, and relates this to the ascent of a twisted Ω-shaped magnetic tube; they pointed out that sunspots in a bipolar pair must rotate in opposite directions. Since only a small part of the sunspot flux is closed in the positive magnetic pole considered, we suppose that the pole can rotate in the opposite direction, around a center of rotation that is located outside.

In all the described events, the rates of flux cancellation are of the order of 10^{19} Mx/h, consistent with [6]. The growth rates of the emerging magnetic flux and the rates of flux decrease during cancellation are also comparable. The rates of magnetic-flux decrease during the formation of a filament were earlier found from MDI magnetograms to be of the order of 10^{19} Mx/h in a quiet region [16] and 10^{21} Mx/h in an active region [2]. In contrast to [2], we have considered each pair event separately; this is partially why our values are smaller.

During the formation of the new part of the filament on October 22, the flux fluctuations are a factor of 1.5–2 lower, and are shorter than in other cases. The emergence of the bipolar pairs "b" and "c" accounts for 70% of the fluctuation of the positive flux in the eastern part of the active region from 16:00 UT October 23 until 14:24 UT October 24 (Fig. 5). It is possible that the events of October 22 and October 23–24 represent developments on larger spatial and temporal scales.

3.5. The Formation of the Axial Magnetic Field in a Filament

The morphology of the emergence of new magnetic flux (bipolar pairs), the disappearance of flux in the region of formation, and development of a filament is interesting in connection with the nature of the axial component of the magnetic field in a filament.

There are two interpretations of the observed flux disappearance.

The first [17] considers the magnetic reconnection of approaching magnetic poles, which modified the magnetic topology such that an axial filament field is gradually formed. We have applied this interpretation in the previous section. Reconnection is favored by the observed long-lived brightening of Hα flocculi above cancellation sites and on the TRACE 171 Å filtergrams. Chae [18] likewise concluded that the series of ejections and eruptions arising at the cancellation site during the formation of a filament are due to reconnection processes. His estimate of the mass of material transported by the observed ejections and eruptions is consistent with the lower limit of the filament mass.

The second interpretation [19] assumes the emergence of a flux tube that has been completely formed below the photosphere. The transfer of the horizontal tube to the upper chromosphere and corona occurs in separate segments, and the cross section of the flux tube at the photosphere level is observed as approaching pairs of magnetic poles and a disappearance of the flux. In this situation, the rates of flux appearance and disappearance should be identical, since they are associated with the same physical process. A similar phenomenon was pointed out in the previous section. Figures 6 and 7 show the initial and subsequent closing of the lines of force, which coincide with the direction of the filament. This may indicate either the reconnection or the presence of a subphotospheric connection between the cancelled poles, i.e., the emergence of a horizontal field tube.

In both cases the decaying flux is comparable to the flux of the axial field in the filament. The observed value of the decaying flux in our and other analyses [2, 16, 18, 20, 21] is from 10^{19} Mx for quiescent filaments to 10^{22} Mx for filaments within active regions. There have been no direct measurements of the axial magnetic field in filaments. In [22], the decaying flux is compared to the estimated magnetic flux in a filament, and is found to be consistent with the above lower limit.

In both interpretations the process of feeding material to a filament is directly connected with the ascent of horizontal flux tubes; in the model of Rust [19], the flux tube is formed completely beneath the photosphere. The existence of a horizontal field in the photosphere, in the region of the filament, is revealed, first, by the elongated structure of fibrils in the filament channel and near the filament [23] and, second, by direct vector magnetograph measurements of the transverse field components [24]. Note that the axial magnetic field of a filament reflects its large-scale structure, and there exist many problems concerning its nature and direction. These have been addressed most comprehensively by Rust and Kumar [25]. Essentially, they postulated the existence of a global toroidal magnetic field beneath the photosphere at middle and high latitudes. The direction of this field is opposite to the direction of the toroidal field at low latitudes, where the current activity cycle develops. This can explain only high-latitude filaments, and cannot explain filaments at low latitudes or large quiescent filaments nearly elongated in the meridional direction. Earlier, we briefly discussed in [24] the possibility of forming large-scale horizontal magnetic fields in subphotospheric layers, along the boundaries of supergranules, by a mechanism of topological pumping [26], and the role of supergranulation motions near polarity-inversion lines of the large-scale magnetic field [4]. This mechanism of magnetic-field formation is possible both in a quiet atmosphere and an active region. Of course, the large-scale topology of a horizontal flux tube is related to the large-scale photospheric field, as well as various types of restructuring under the action of the photospheric plasma flows.

A more complete understanding of filament formation will require further development of vector magnetograph measurements of the magnetic field in the photosphere and chromosphere and analysis of the structure of EUV maps. Studies of the initial stages of the formation of filaments and their channels are especially important.

4. CONCLUSIONS

(1) We have confirmed our earlier result [4, 24] that filaments are formed at the boundaries of supergranules in the regions of polarity-inversion lines.

(2) The result of Chae [11] that sinistral filaments have a positive magnetic chirality is confirmed.

(3) We have obtained new information on cancellation processes, and have studied the cancellation of new and old fluxes. Our estimates of the cancelled flux are within the limits obtained by other researchers. The direction of motion of the cancelling magnetic poles and their positional relationship testify that the

axial field of the filament formed either via the reconnection of the cancelling magnetic poles or due to the emergence of a horizontal magnetic flux tube.

ACKNOWLEDGMENTS

The authors are grateful to working groups of the ground-based Big Bear, Catania, Meudon, Huairou, Kanzelhöhe, Learmonth, and Hida observatories, as well as to the SOHO/MDI, SOHO/EIT, and TRACE teams, for granting access to their Internet databases. We also thank colleagues from our Institute for the opportunity to use the IDL software. This work was supported by the Program of Support of Leading Scientific Schools of the Russian Federation (grant no. NSh-733.2003.2), the Integration Project of the Siberian and Far-Eastern Divisions of the Russian Academy of Sciences, and the Program for Basic Research of the Presidium of the Russian Academy of Sciences on Solar Activity and Physical Processes in the Sun–Earth System.

REFERENCES

1. Y. Jiang and J. Wang, Astron. Astrophys. **356**, 1055 (2000).
2. J. Chae, Astrophys. J. **560**, 476 (2001).
3. B. Schmieder, N. Mein, Y. Deng, et al., Sol. Phys. **223**, 119 (2004).
4. M. Grigor'ev, L. V. Ermakova, and A. I. Khlystova, Astron. Zh. **81**, 64 (2004) [Astron. Rep. **48**, 58 (2004)].
5. S. H. B. Livi, J. Wang, and S. F. Martin, Austral. J. Phys. **38**, 855 (1985).
6. S. F. Martin, S. H. B. Livi, and J. Wang, Austral. J. Phys. **38**, 929 (1985).
7. K. L. Harvey, H. P. Jones, C. J. Schrijver, and M. J. Penn, Sol. Phys. **190**, 35 (1999).
8. Y. E. Litvinenko and S. F. Martin, Sol. Phys. **190**, 45 (1999).
9. F. Martin, Sol. Phys. **182**, 107 (1998).
10. S. F. Martin, *Coronal and Prominence Plasmas*, Ed. by A. I. Poland, NASA Conf. Publ. No. 2442, p. 73 (1986).
11. J. Chae, Astrophys. J. Lett. **540**, L115 (2000).
12. C. Zwaan, Sol. Phys. **60**, 213 (1978).
13. R. A. Shine, G. W. Simon, and N. E. Hurlburt, Sol. Phys. **193**, 313 (2000).
14. *Solar Vector Magnetograms 2001* (Solar Activity World Data Center, National Astronomical Observatory of Japan, 2002).
15. D. S. Brown, R. W. Nightingale, D. Alexander, et al., Sol. Phys. **216**, 79 (2003).
16. P. Wood and P. Martens, Sol. Phys. **218**, 123 (2003).
17. P. C. Martens and C. Zwaan, Astrophys. J. **558**, 872 (2001).
18. J. Chae, Astrophys. J. **584**, 1084 (2003).
19. D. M. Rust, J. Geophys. Res. **106**, 25 075 (2001).
20. J. Chae, C. Denker, T. J. Spirock, et al., Sol. Phys. **195**, 333 (2000).
21. J. Chae, Y. Moon, H. Wang, and H. S. Yun, Sol. Phys. **207**, 73 (2002).
22. J. L. Leroy, V. Bommier, and S. Sahal-Brechot, Sol. Phys. **83**, 135 (1983).
23. S. F. Martin, R. Bilimoria, and P. W. Tracadas, *Solar Surface Magnetisms* (Springer-Verlag, New York, 1994), p. 303.
24. V. M. Grigoryev and L. V. Ermakova, Astron. Astrophys. Trans. **17**, 355 (1999).
25. D. M. Rust and A. Kumar, Sol. Phys. **155**, 69 (1994).
26. E. M. Drobyshevski and V. S. Yuferev, J. Fluid Mech. **65**, 38 (1974).

Translated by G. Rudnitskiĭ